coatings

MDPI

Article

Study on High Temperature Properties of Yttrium-Modified Aluminide Coating on K444 Alloy by Chemical Vapor Deposition

Hanzhe Yang, Yong Wu, Qingyun Sun *, Fu Yang, Chunhuai Xia, Siyao Xia and Jianrong Du

China Academy of Machinery Wuhan Research Institute of Materials Protection Co., Ltd., Wuhan 430030, China; yanghz98@126.com (H.Y.); wuyong@rimp.com.cn (Y.W.); fyangrimp@163.com (F.Y.); xch863@163.com (C.X.); xiasiyao@126.com (S.X.); xiaojianjian2024@163.com (J.D.)

* Correspondence: sqysunqingyun@163.com

Abstract: This work aims to explore a method of improving the high-temperature oxidation resistance and thermal corrosion resistance of a hollow blade of gas turbine. The yttrium-modified aluminide coating was prepared on the surface of nickel-based superalloy K444 by chemical vapor deposition (CVD). The microstructure, high temperature oxidation resistance, and thermal corrosion resistance of the modified aluminide coating deposited at 950 °C, 1000 °C, and 1050 °C were compared. The microstructure and morphology of the coatings were observed and analyzed by XRD, SEM, and EDS. The results showed that adding yttrium and changing the deposition temperature had no effect on the double-layer structure (outer layer and diffusion layer) of the coating. Compared with adding yttrium, the deposition temperature had a greater effect on the coating thickness. When the deposition temperature was 1050 °C and the deposition time was 2 h, the thickness of the yttrium-modified aluminide coating increased by 33% compared to that of a single aluminide coating. The high temperature oxidation resistance and thermal corrosion resistance of the three groups of yttrium-modified aluminide coatings are better than that of the single aluminide coating. The resistance to high temperature oxidation and hot corrosion of the yttrium-modified aluminide coating deposited at 1050 °C was better than that of yttrium-modified aluminide coating deposited at 1000 °C, and both were better than that of the modified coating deposited at 950 °C. The higher the deposition temperature, the higher the yttrium content of the coating, the faster the film-forming speed of α-Al_2O_3, and the better the high temperature oxidation resistance and thermal corrosion resistance of the coating.

Keywords: chemical vapor deposition; modified aluminide coating; high temperature oxidation; salt-coated thermal corrosion

Citation: Yang, H.; Wu, Y.; Sun, Q.; Yang, F.; Xia, C.; Xia, S.; Du, J. Study on High Temperature Properties of Yttrium-Modified Aluminide Coating on K444 Alloy by Chemical Vapor Deposition. *Coatings* **2024**, *14*, 750. https://doi.org/10.3390/coatings14060750

Academic Editor: Michał Kulka

Received: 14 May 2024
Revised: 8 June 2024
Accepted: 12 June 2024
Published: 13 June 2024

1. Introduction

The K444 nickel-based superalloy is widely used in core hot end components, such as large guide and turbine blades, because of its excellent high temperature oxidation resistance, corrosion resistance, and outstanding high temperature creep strength and fracture strength [1–4]. It has been selected as stage 1 to stage 4 turbine blade material for R0110 heavy duty gas turbines [5]. With the development of the aviation and navigation industries, high temperature oxidation and thermal corrosion in the inner cavity of gas turbine blades have become the main factors limiting their service life [6,7]. One effective way to solve these problems is to prepare aluminide coating on the surface of gas turbine blade cavity passage [8,9]. The chemical vapor deposition (CVD) method can realize the internal aluminizing of complex parts by gas reaction, and the infiltrating agent does not have direct contact with the substrate, which has little influence on the workpiece [10,11]. The CVD method can control the coating element content and coating thickness by controlling the reaction gas flow and deposition time, which makes it easy to control the reaction process, thus it has been widely used in the preparation of aluminide coatings in recent years [12]. However, the single aluminide coating is easy to crack and flake, it is brittle

and sensitive to S, and has a fast degradation rate, all of which limit its use. Adding a small amount of Y to the aluminide coating can reduce the oxidation rate in the system, improve the adhesion of the oxide film, and improve the resistance to high temperature oxidation and hot corrosion of the coating. This may be due to the fact that segregation of yttrium element at the grain boundary can block or cut off the short-circuit diffusion channel to a certain extent, inhibiting the outward diffusion of Cr, Ti and other elements and inhibiting the inward diffusion of the S element [13,14]. Zielińska M et al. [15] prepared a βNiAl coating on the nickel-based superalloy Mar M247 with the CVD method, and studied its high temperature oxidation properties through the cyclic oxidation test. The results show that the weight gain of aluminide-coated samples is less. Dun [16] from the Wuhan Institute of Materials Protection successfully achieved Al–Y co-diffusion on the surface of the lnconel 718 nickel-based superalloy with the CVD method, and prepared dense and uniform yttrium-modified aluminide coating. The effects of yttrium on the thermal shock properties and high temperature oxidation resistance of the aluminide coating were studied.

At present, there are few comparative studies on the high temperature properties of yttrium-modified aluminide coatings at different deposition temperatures. Therefore, in this paper, a chemical vapor deposition method was used to prepare three kinds of yttrium-modified aluminide coatings at three deposition temperatures (950 °C, 1000 °C, and 1050 °C) on the surface of a K444 nickel-based superalloy, and the cyclic oxidation experiment at 1100 °C and the salt coating thermal corrosion test at 900 °C-NaCl + Na_2SO_4 werealso performed. The effect of deposition temperature and yttrium on the high temperature performance of the coatings was investigated by comparing their properties.

2. Experimental Materials and Methods

The K444 nickel-based superalloy was used in the experiment as a sample, and the nominal composition is shown in Table 1. The cuboid sample size was processed as 20 mm × 10 mm × 5 mm, and a small hole with a diameter of 1 mm was punched at one end near the edge for easy hanging. In this paper, an MP-2B metallographic sample grinding and polishing machine, produced by Guangzhou Weiyee, China, was used, with a maximum speed of 1000/min. Diamond spray from China Apu was selected as polishing agent. First, the sample was polished with 400-mesh, 800-mesh, 1200-mesh abrasive papers and a polishing agent, in turn, with the polishing machine, to remove the oxide film on its surface, then the oil was removed by ultrasonic cleaning with acetone, and finally, the sample was cleaned by ultrasonic cleaning with anhydrous ethanol and dried for use.

Table 1. Nominal composition of K444 nickel-based superalloy.

Element	C	Cr	Co	Mo	Al	B	Ti	W	Ni	Hf	Nb
Content/wt.%	0.05	15.28	10.48	2.08	3.10	0.08	4.40	5.13	Residue	0.31	0.19

The yttrium-modified aluminide coating was prepared on the surface of the K444 alloy using a one-step method (both Y and Al were deposited in one experiment at the same time) with hot-wall chemical vapor deposition (hot-wall CVD) equipment. A picture of the real equipment is shown in Figure 1; 33YAl-66AlCr-1NH_4Cl was used as the precursor, in which a yttrium–aluminum alloy (yttrium mass fraction 85%) was used as the yttrium supply agent, and an aluminum–chromium alloy (aluminum mass fraction 50%) was used as the aluminum supply agent. The reaction gas was HCl, the deposition time was 2 h, and the deposition temperatures were 950 °C, 1000 °C, and 1050 °C.

Figure 1. Picture of CVD real equipment.

The coating preparation process is mainly divided into three steps:

(1) H_2 as the current carrying gas and HCl are fed into the mixing tank;
(2) HCl reacts with the precursor in the external generator to produce $AlCl_n$ and YCl_n (n = 1, 2, 3);
(3) Gaseous halides enter the deposition chamber, release active atoms on the sample surface, and deposit and diffuse to form yttrium-modified aluminide coatings.

Cyclic oxidation tests and salt corrosion tests were carried out in a muffle furnace in static air. The KJ-M1400 muffle furnace from Kejia in Zhengzhou, China, with a power of 155 kW and a maximum heating temperature of 1400 °C, was used. The cyclic oxidation test process referred to the aviation industry standard of China "determination method for oxidation resistance of steels and high temperature alloys" [17], and the test temperature was 1100 °C. When the temperature of the muffle furnace was stable at 1100 °C, the samples were immediately placed in the furnace, held for 1 h, and then taken out for air cooling for 10 min. The above operation was a cycle, and a total of 100 cycles were performed. The samples of each group were weighed at the 1st, 4th, 7th, and 10th cycles. After 10 cycles, the samples were weighed again every 10 cycles. The peeling oxide skin was left to fall off naturally and was not included in the weight. After the test was completed, the mass change per unit area was obtained by dividing the weight change by the specimen surface area.

The salt coating corrosion test process referred to the aviation industry standard of China "test for corrosion behaviors at high-temperature with corrosive salts" [18], and the test temperature was 900 °C. First, a concentrated salt coating brine mixed with 95 wt.% Na_2SO_4 and 5 wt.% NaCl was sprayed onto the surface of the sample with a spray bottle. The salt concentration was 100 g/L, and the salt amount was 2.5–3.5 mg·cm^{-2}. Then the sample was dried and heated in the muffle furnace to 900 °C, held for 10 h, and air cooled to room temperature. Finally, the sample was cleaned with deionized water to remove the residual salt film, then dried and weighed. The above operation was a cycle, and this test lasted 50 h in five cycles. In this paper, the FA224 multifunctional electronic balance which index value is 0.0001 g produced by Lichen Instrument Technology Co., Ltd. (Shaoxing City, China) was used.

Three kinds of yttrium-modified aluminide coatings after oxidation and corrosion were characterized. The phase composition of the coatings was analyzed by X-ray polycrystalline diffractometer, and the cross-section morphology and element content of the coatings were observed by scanning electron microscope and EDS spectrometer. In this paper, The Japanese Rigaku XRD SmartLab intelligent X-ray polycrystalline diffractometer was used (Haidian District, Beijing, China), with a rated output power of 3 kW. Cu was used as the target, and the corresponding wavelength of the X-ray was 0.154056 nm. The measurement

angle was 10°~90°, and the measurement rate was 8°/min. The JSM-6510LV scanning electron microscope of Japan Electronics Co., Ltd. (Xicheng District, Beijing, China), with a resolution of 3 nm, with the JINCAx-actSN 57014 EDS spectrometer, was used.

3. Experimental Results and Analysis

3.1. Coating Composition and Structure

Figure 2 shows the XRD patterns of a single aluminate coating on the K444 alloy deposited at 1050 °C and three kinds of yttrium-modified aluminate coatings on the K444 alloy deposited at 950 °C, 1000 °C, and 1050 °C. The characteristic peaks of the four coatings are similar, mainly β-NiAl and NiFe phases, indicating that adding yttrium and changing the deposition temperature has little effect on the surface structure of the coating.

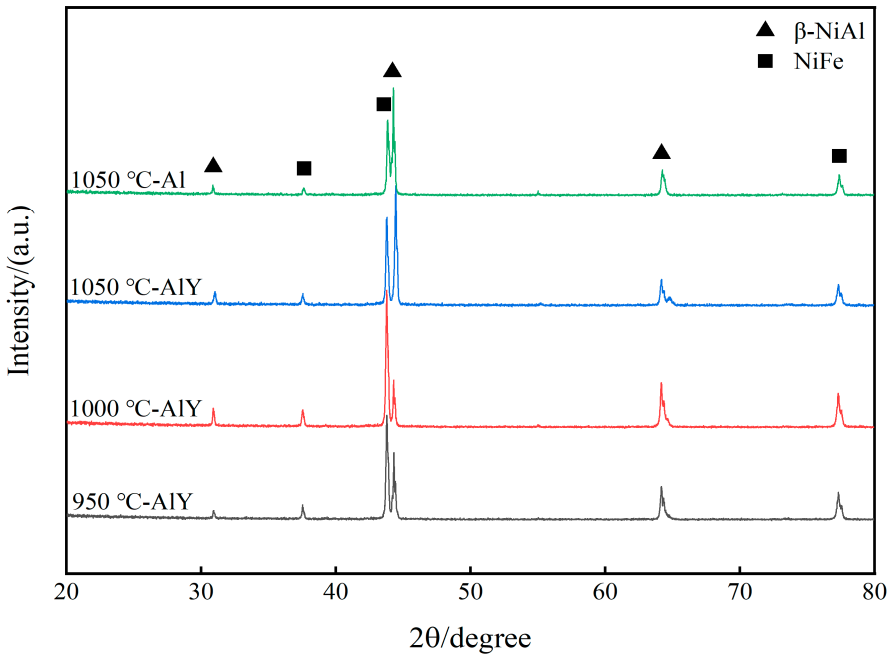

Figure 2. XRD patterns of single aluminide coating and three kinds of yttrium-modified aluminide coatings.

Figure 3 shows the cross-sectional microstructure of (a) the single aluminide coating and (b) the yttrium-modified aluminide coating on the K444 alloy deposited at 1050 °C and element line scan maps of Al, Ti, Co, Ni, Cr, and Y. The direction of arrows in the Figure 3a,b indicates the element line scanning direction. The deposition time of the two groups was 2 h, and the deposition temperature was 1050 °C. It can be seen from the figure that both groups of coatings have two layers, the outer layer and the diffusion layer. The thickness of the single aluminide coating is about 20 μm, and that of the yttrium-modified aluminide coating is about 28 μm. It can be seen from element line scan maps that the Al of the yttrium-modified aluminide coating is more widely distributed, while the external diffusion degree of Ti and Cr is lower than that of single aluminide coating, indicating that the addition of yttrium can promote the internal diffusion of Al atoms, hinder the external diffusion of Ti, Cr, and other matrix elements, and increase the coating thickness.

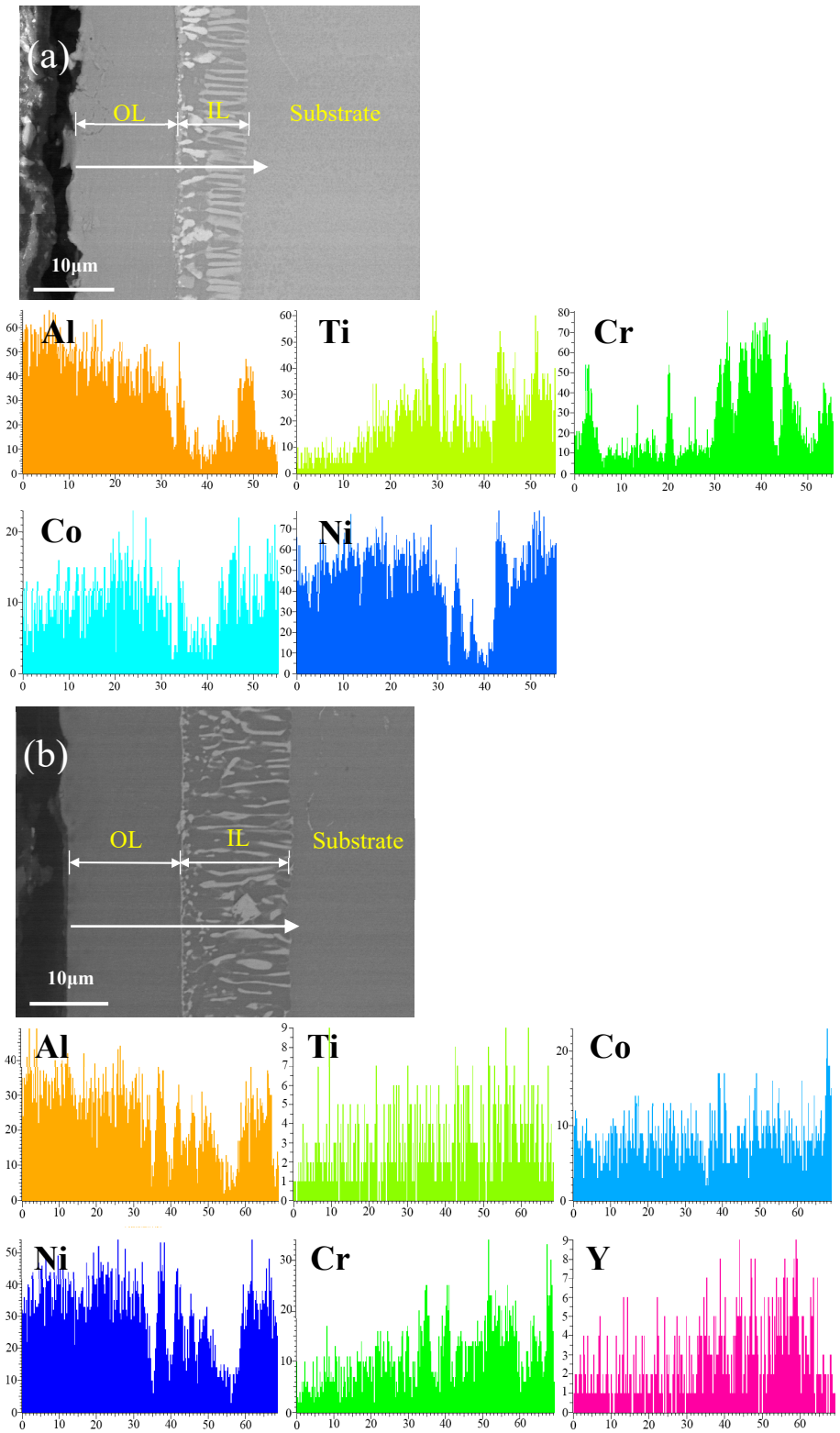

Figure 3. Cross-sectional microstructure of (**a**) single aluminide coating and (**b**) yttrium-modified aluminide coating on K444 alloy deposited at 1050 °C and element line scan maps of Al, Ti, Co, Ni, Cr, Y.

Figure 4a–c show the cross-sectional microstructure of yttrium-modified aluminide coatings on the K444 alloy deposited at 950 °C, 1000 °C, and 1050 °C. The number 1 in the Figure 4a–c represents the zone of outer layer and the number 2represents the zone of interdiffusion layer. The coatings of the three groups are all double-layer structures, with an outer layer and a diffusion layer. Among them, the thickness of the yttrium-modified aluminide coating deposited at 1050 °C is the biggest, about 28 μm, the thickness of the coating deposited at 1000 °C is about 15 μm, and the thickness of the coating deposited at 950 °C is the smallest, about 10 μm. The principle of aluminide coating prepared by chemical vapor deposition is mainly the internal diffusion of Al and the external diffusion of Ni [19,20], and the outer layer is mainly composed of Al and Ni. The inner layer is an interdiffusion zone, and the bright white area is a Cr-rich phase [21]. Figure 5 shows the distribution curves of yttrium in three groups of yttrium-modified aluminide coatings, corresponding to zone 1 and 2 of the three groups of coatings in Figure 4. The yttrium in the three groups was distributed evenly, and the content in the outer layer of the coating was slightly higher than that in the diffusion layer. The content of yttrium in the yttrium-modified aluminide coating deposited at 1050 °C was the highest (0.85 wt.% as a result of line scanning), the content of yttrium in the yttrium-modified aluminide coating deposited at 1000 °C was less (0.75 wt.% as a result of line scanning), and the content of yttrium in the yttrium-modified aluminide coating deposited at 950 °C was the least (0.245 wt.% as a result of line scanning). According to research [22], the addition of yttrium can accelerate the deposition rate of active aluminum atoms, increase the content of aluminum in the coating, and increase the coating thickness. The higher the deposition temperature, the faster the reaction rate and the more yttrium content in the coating. Under the influence of deposition temperature and yttrium, the diffusion rate of aluminum element is further accelerated, and the coating thickness is further increased.

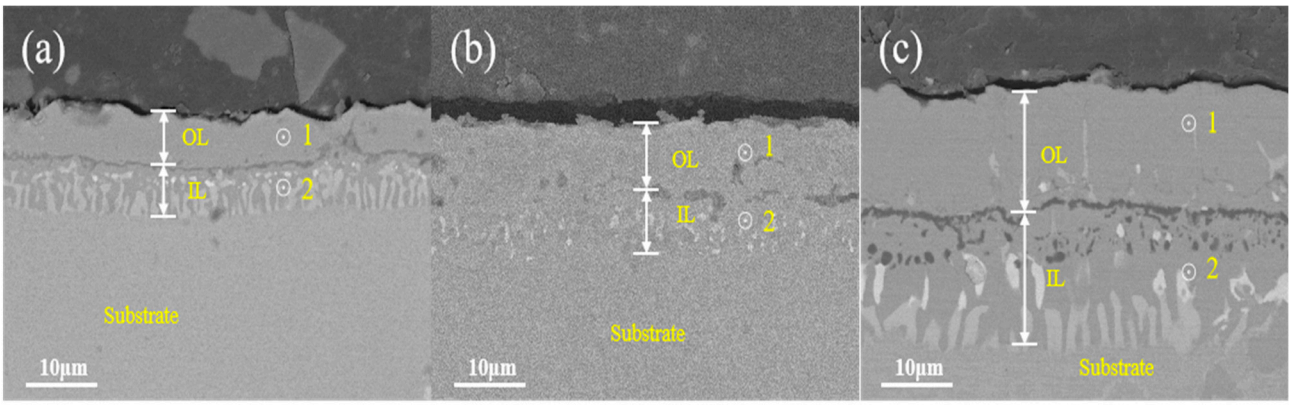

Figure 4. Cross-sectional microstructure of yttrium-modified aluminate coatings deposited at (**a**) 950 °C, (**b**) 1000 °C, and (**c**) 1050 °C on K444 alloy.

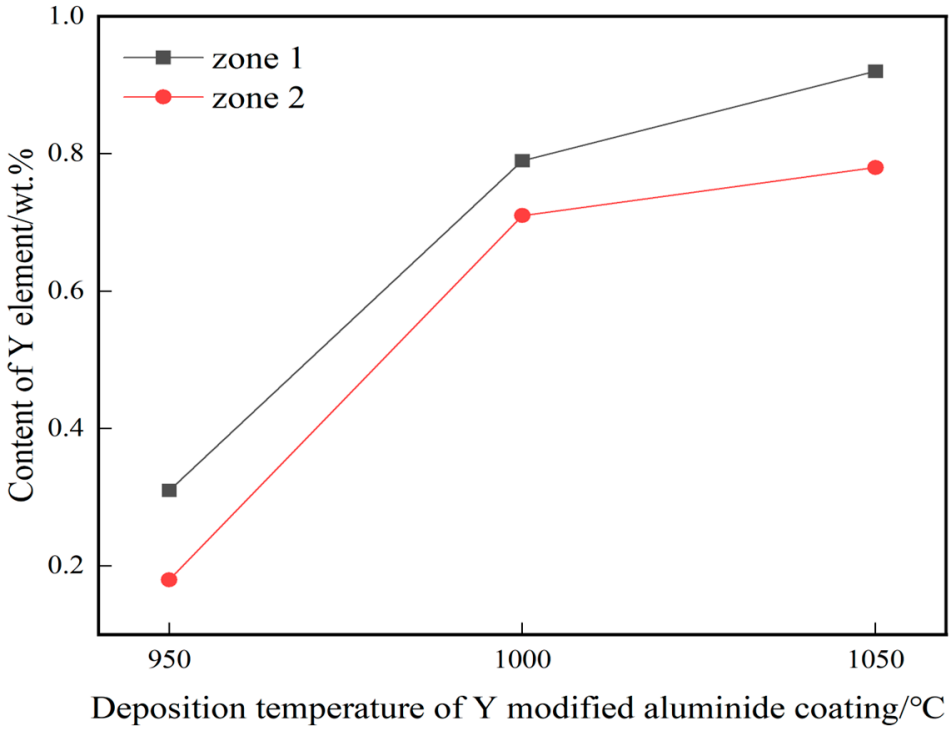

Figure 5. Distribution of Y in the three groups of yttrium-modified aluminide coatings on K444 alloy.

3.2. Cyclic Oxidation Behavior of Coating

Figure 6 shows the kinetics curves of the single aluminide coating deposited at 1050 °C and the three groups of yttrium-modified aluminide coating deposited at 950 °C, 1000 °C, and 1050 °C of cyclic oxidation for 100 h at 1100 °C. It can be seen that the single aluminide coating and the three groups of yttrium-modified aluminide coating gain weight faster from 0–10 h, and the β-NiAl in the coating quickly forms a dense Al_2O_3 film, and after 10 h, the weight gain is slow, indicating that a complete Al_2O_3 film has been formed on the surface of the coating to protect the matrix from further oxidation. The weight gain of the single aluminide coating was 0.55 mg·cm^{-2}, the weight gain of the yttrium-modified aluminide coating deposited at 1050 °C was 0.3 mg·cm^{-2}, and the resistance of the coating to high temperature oxidation was increased by 45%. The weight gain of the three groups of yttrium-modified aluminide coatings is slower than that of the single aluminide coating, indicating that the high temperature oxidation resistance of the yttrium-modified aluminide coating is better than that of the single aluminide coating. Compared with the three groups of yttrium-modified aluminide coatings, the weight gain of the yttrium-modified aluminide coating deposited at 950 °C is the largest, indicating that its oxide film has a greater tendency to crack and flake, and its oxidation resistance at high temperature is poor. The slope of the weight gain curve of the modified coating deposited at 1000 °C and 1050 °C is similar, indicating that the resistance of the two coatings to high temperature oxidation tends to be consistent.

Figure 7 shows the XRD patterns of single aluminide coating deposited at 1050 °C and three groups of yttrium-modified aluminide coating deposited at 950 °C, 1000 °C, and 1050 °C on K444 alloy after cyclic oxidation for 100 h at 1100 °C. The oxidized aluminide coatings are mainly Al_2O_3, TiO_2, and γ-Ni_3Al phases, and the yttrium-modified aluminide coatings are Al_2O_3, TiO_2, γ-Ni_3Al, and β-NiAl phases. This indicates that part of the aluminum in the coating is consumed by oxidation, and the β-NiAl phase is transformed into the more brittle γ-Ni_3Al phase. There is a γ-Ni_3Al phase in the single aluminide coating, but no β-NiAl phase, which shows that the coating damage is more serious.

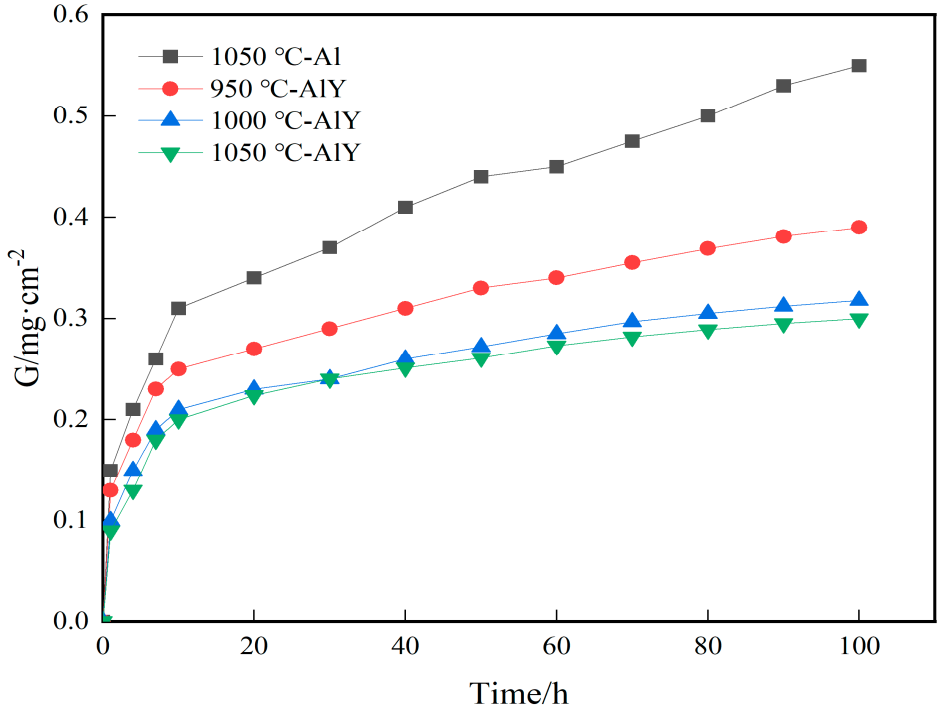

Figure 6. Oxidation kinetics of single aluminide coating and three groups of yttrium-modified aluminide coatings on K444 alloy.

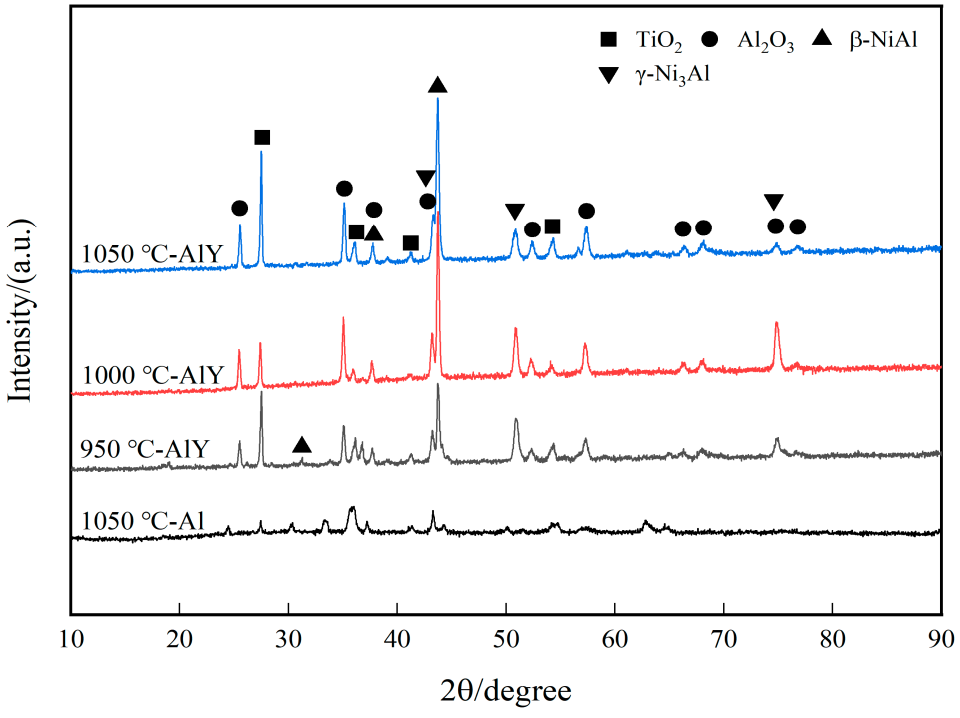

Figure 7. XRD patterns of single aluminide coating and three groups of yttrium-modified aluminide coatings on K444 alloy after cyclic oxidation at 1100 °C for 100 h.

Figure 8 shows the cross-sectional microstructure of a single aluminide coating and a yttrium-modified aluminide coatings deposited at 950 °C, 1000 °C, and 1050 °C on the K444 alloy, and element line scan maps of Al, Ti, O, Ni, Cr, and Y after cyclic oxidation for 100 h at 1100 °C. The direction of arrows in the Figure 8a–d indicates the element line scanning direction. As can be seen from the Figures 7 and 8, the outer layer of a single aluminide coating is mainly NiO compounds and Cr_2O_3, and the inner layer is TiO_2. The outer layer

of the modified coating deposited at 950 °C is mainly Cr_2O_3, and the inner layer is Al_2O_3 and TiO_2. The outer layer of the modified aluminide coating deposited at 1000 °C is Al_2O_3, TiO_2, and the inner layer is Cr_2O_3. The outer layer of the modified aluminide coating deposited at 1050 °C is Al_2O_3, Cr_2O_3, and the inner layer is TiO_2. The outer layer of the single aluminide coating is undulating, the content of Ni is high, the oxide layer is peeling off, and the local failure of the coating is serious. The outer layer of the modified aluminide coating is relatively flat, among which the oxidation product layer of the yttrium-modified coating deposited at 950 °C is thicker, about 14.3 μm, and the oxidation product of the coating deposited at 1000 °C and 1050 °C is thinner than that of the coating deposited at 950 °C, about 2 μm. The yttrium-modified aluminide coating deposited at 1000 °C and 1050 °C has dense surface oxide film, therefore it has good high-temperature oxidation resistance. The high-temperature oxidation resistance of the yttrium-modified aluminide coating is better than that of single aluminide coating, and the high temperature oxidation resistance of the modified aluminide coating deposited at 1000 °C and 1050 °C is similar, but is better than that of modified aluminide coating deposited at 950 °C.

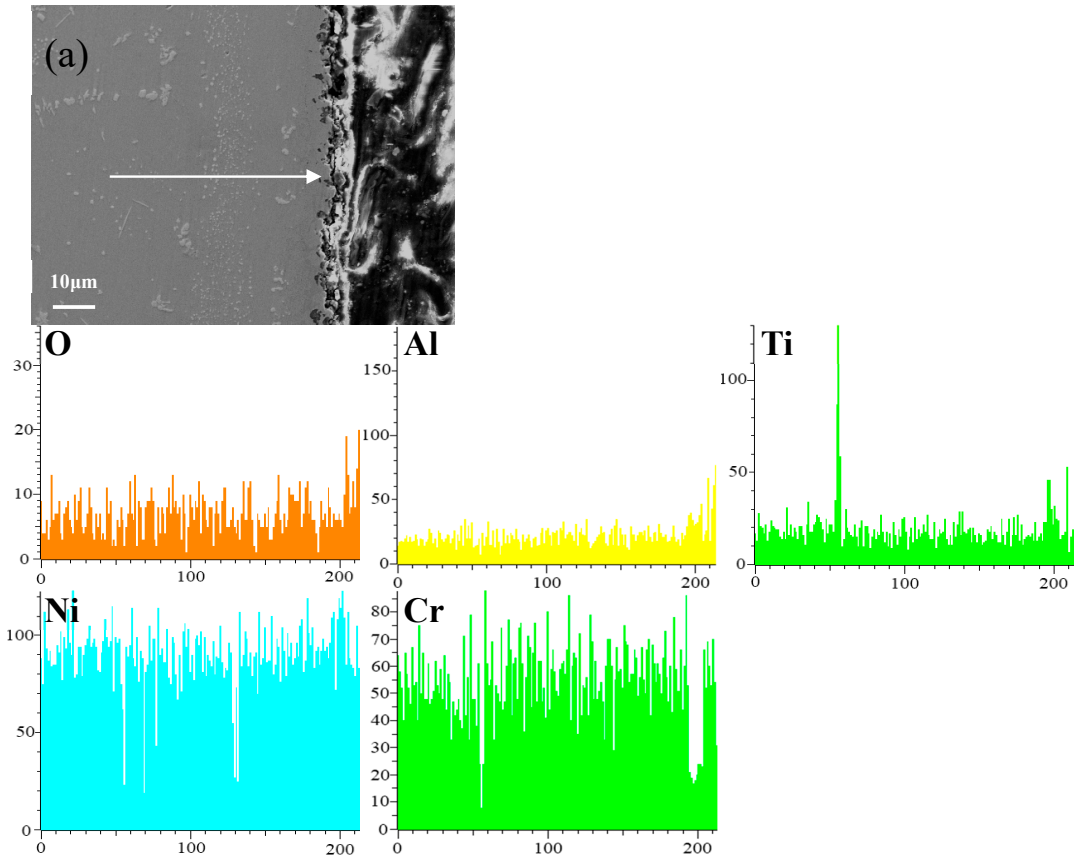

Figure 8. *Cont.*

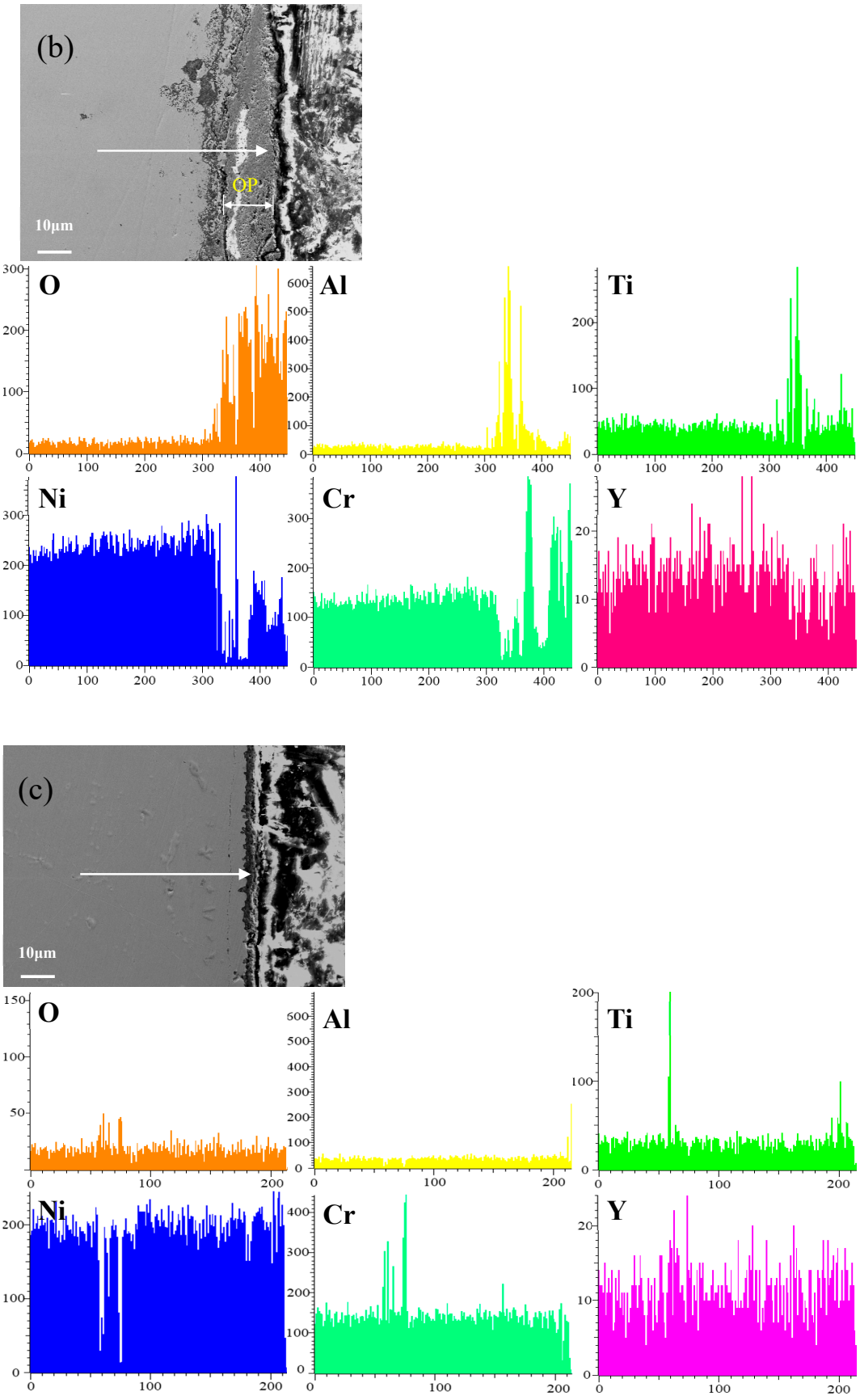

Figure 8. *Cont.*

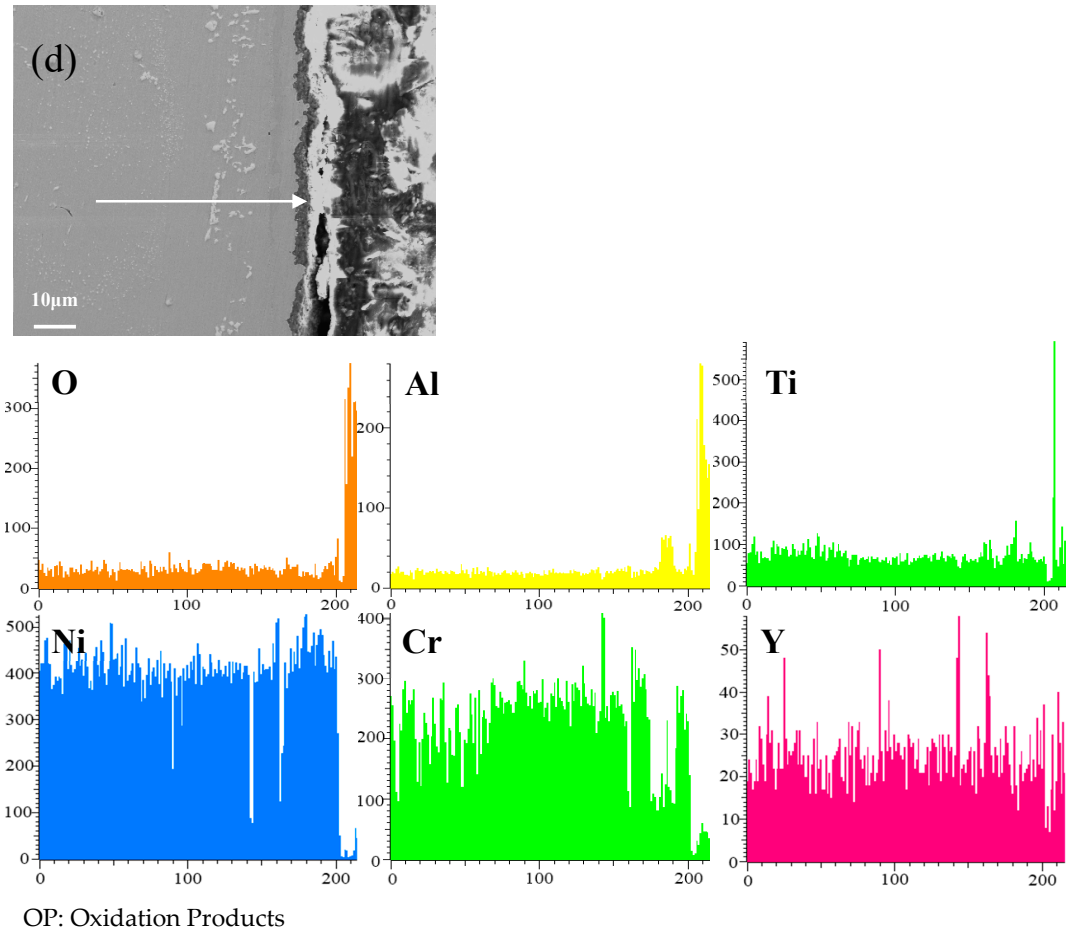

Figure 8. Cross-sectional microstructure of (**a**) single aluminide coating and yttrium-modified aluminide coatings deposited at (**b**) 950 °C, (**c**) 1000 °C, and (**d**) 1050 °C and element line scan maps of Al, Ti, O, Ni, Cr, Y on K444 alloy after cyclic oxidation for 100 h at 1100 °C.

Figure 9 shows the surface morphologies of the single aluminide coating and three groups of yttrium-modified aluminide coatings on the K444 alloy after cyclic oxidation for 100 h at 1100 °C, where (a) is single aluminide coating deposited at 1050 °C. (b), (c) and (d) are three groups of yttrium-modified aluminide coatings on the K444 alloy deposited at 950 °C, 1000 °C, and 1050 °C. Both the single aluminide coating and the yttrium-modified aluminide coating deposited at 950 °C have hole defects, but the single aluminide coating has more defects. The modified coatings deposited at 1000 °C and 1050 °C are denser.

Table 2 shows the EDS surface scan element content table of single aluminide coating and three groups of yttrium-modified aluminide coatings on the K444 alloy, corresponding to Figure 9a–d. It can be seen that the atomic proportion of Al + O on the surface of the four groups of coatings is more than 80%. The single aluminide coating and the modified aluminide coating deposited at 950 °C have more types of swept elements, including Co and Fe, the content of Co is 1.82 wt.% and 0.86 wt.%, and the content of Fe is 3.18 wt.% and 2.36 wt.%, indicating that the coating has a certain degree of damage. However, no Co was detected on the surface of modified coating deposited at 1000 °C, the matrix element types were less, the content was lower (Fe content was 0.34 wt.%), and the oxidation resistance was excellent. Substrate element types of yttrium-modified coating deposited at 1050 °C are the least, and Co and Fe are not detected, so the oxidation resistance is the best.

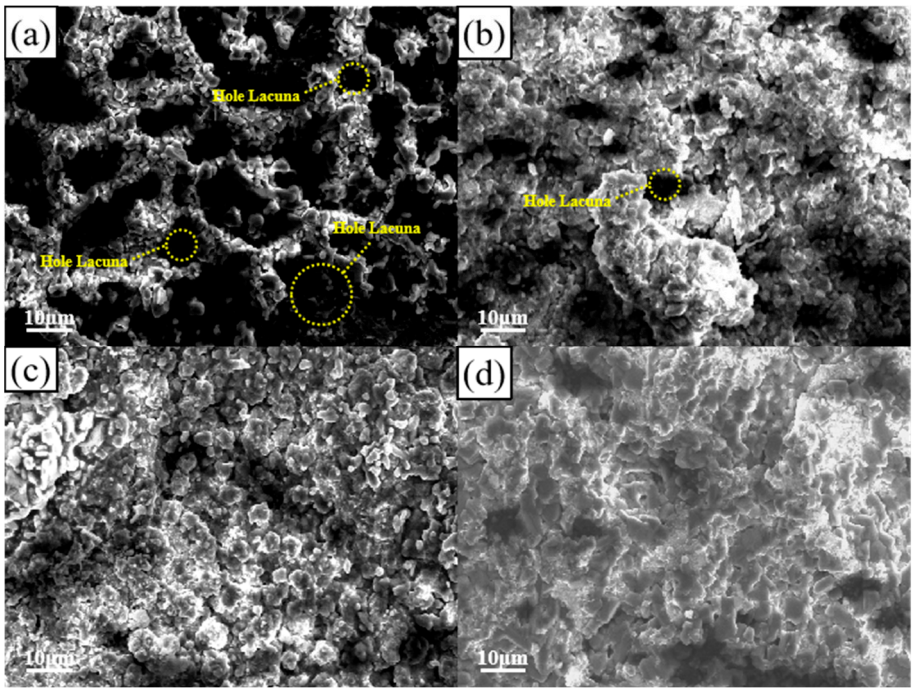

Figure 9. Surface morphologies of (**a**) single aluminide coating and yttrium-modified aluminide coatings deposited at (**b**) 950 °C, (**c**) 1000 °C, and (**d**) 1050 °C on K444 alloy after cyclic oxidation at 1100 °C for 100 h.

Table 2. Surface scan element content table of single aluminide coating and three groups of yttrium aluminide coatings on K444 alloy after cyclic oxidation for 100 h (wt.%).

Coatings \ Element	O	Al	Ni	Cr	Ti	Co	Fe
1050 °C-Al	65.82	15.76	0.32	0.66	12.43	1.82	3.18
950 °C	66.40	19.03	2.97	2.43	5.34	0.86	2.36
1000 °C	67.04	25.33	0.53	0.89	5.87	—	0.34
1050 °C	67.40	25.57	0.69	0.43	5.96	—	—

The coating surface of single aluminide coating and three groups of yttrium-modified aluminide coatings is the β-NiAl phase, and the metastable cubic crystal Al_2O_3, including γ phase, δ phase and θ phase, is first formed during oxidation. As the oxidation process continues, these metastable Al_2O_3 will gradually transform into stable α-Al_2O_3. Studies have shown that [23,24] rare earth elements can promote the nucleation of steady-state α-Al_2O_3 by forming oxidation particles, thus promoting the transition from metastable Al_2O_3 to stable Al_2O_3. In addition, rare earth elements can also reduce the critical Al content of Al_2O_3 film formation on the surface, reduce the critical concentration of Al_2O_3 formation on the surface, and extend the deposition time of the coating. Therefore, more yttrium can better promote the formation of the α-Al_2O_3 film, thereby improving the high-temperature oxidation resistance of the coating.

3.3. Thermal Corrosion Behavior of Coatings

Figure 10 shows the corrosion weight gain kinetics curves of the single aluminide coating and three groups of yttrium-modified aluminide coatings on the K444 alloy after corrosion at 900 °C-Na_2SO_4 + NaCl for 75 h. The single aluminide coating gained weight rapidly in the early stage of corrosion (0–20 h), reaching 0.0265 mg·cm^{-2} at 20 h. It remained stable in the middle stage of corrosion (20–40 h), gaining 0.0293 mg·cm^{-2} at 30 h. At the later stage of corrosion (40–75 h), the weight gain decreased rapidly, reaching 0.0108 mg·cm^{-2}

at 75 h. The corrosion weight gain of the three groups of modified coatings showed an approximate change law, that is, the weight gain was faster in the initial stage of corrosion (0–10 h), and the rate tended to be stable as time went on. The yttrium modified aluminide coating deposited at 1050 °C had the least corrosion weight gain (0.0100 mg·cm^{-2} at 75 h), and the sample deposited at 950 °C had the most corrosion weight gain (0.0151 mg·cm^{-2} at 50 h), and there was a trend of weight loss at 50–75 h. The weight gain decreased from 0.0151 mg·cm^{-2} to 0.0133 mg·cm^{-2}, indicating that the yttrium-modified coating deposited at 950 °C was seriously corroded. The corrosion weight gain of the three groups of yttrium-modified aluminide coatings was smaller than that of the single aluminide coating, indicating that the thermal corrosion resistance of the yttrium-modified aluminide coating is better than that of the single aluminide coating. The corrosion weight gain of the two groups of modified aluminide coatings deposited at 1000 °C and 1050 °C kept a slow growth trend, indicating that the coating has a good protection effect. The thermal corrosion resistance of the modified coating deposited at 1000 °C and 1050 °C is close, and better than that deposited at 950 °C. The modified aluminide coating with more yttrium content has better resistance to high temperature corrosion.

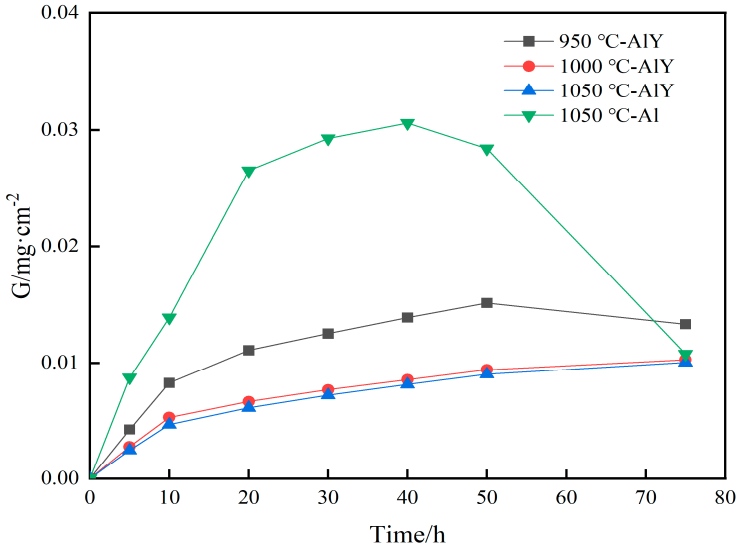

Figure 10. Corrosion kinetics of single aluminide coating and three groups of yttrium-modified aluminide coatings on K444 alloy after corrosion at 900 °C-Na_2SO_4 + NaCl for 75 h.

Figure 11 shows the XRD patterns of single aluminide coating and three groups of yttrium-modified aluminide coatings on the K444 alloy after corrosion at 900 °C-Na_2SO_4 + NaCl for 75 h. It was found that the single aluminide coating has Al_2O_3, Cr_2O_3, and γ-Ni_3Al phases, but no β-NiAl phase, which shows that the coating damage is more serious. The structure of the three groups of modified aluminide coatings is similar, with Al_2O_3, TiO_2, Cr_2O_3, β-NiAl and γ-Ni_3Al phases, indicating that the three groups of modified coatings still have a good function of protecting the internal matrix.

Figure 12 shows the cross-sectional microstructure of single aluminide coating and yttrium-modified aluminide coatings deposited at 950 °C, 1000 °C, and 1050 °C and element line scan maps of Al, Ti, O, Ni, Cr, and S on the K444 alloy after corrosion at 900 °C-Na_2SO_4 + NaCl for 75 h. The direction of arrows in the Figure 12a–d indicates the element line scanning direction. Figure 12a is single aluminide coating deposited at 1050 °C, (b), (c), and (d) are the three groups of yttrium-modified aluminide coatings on the K444 alloy deposited at 950 °C, 1000 °C, and 1050 °C. As can be seen from this figure, the outer layer of the single aluminide coating and the yttrium-modified coating deposited at 950 °C are mainly NiO compounds, and the inner layer is Al_2O_3, Cr_2O_3, and TiO_2. The content of S in the matrix is relatively high, internal vulcanization occurs, and the coating is seriously damaged.

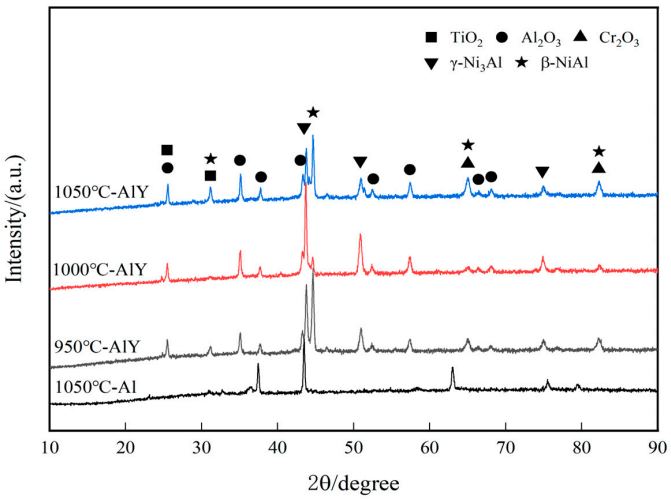

Figure 11. XRD patterns of single aluminide coating and three groups of yttrium-modified aluminide coatings on K444 alloy after corrosion at 900 °C-Na_2SO_4 + NaCl for 75 h.

Figure 13 shows the thickness curves of the corrosion products of the K444 alloy with single aluminide coating and three groups of yttrium-modified aluminide coatings after salt hot corrosion for 75 h. The thickness of the corrosion product of the single aluminide coating is about 29.3 μm, the corrosion product appears in the matrix, and the local damage of the coating is serious. The thickness of the corrosion products of the yttrium-modified aluminide coating deposited at 950 °C is about 26.8 μm, the thickness of the corrosion products of the modified coating deposited at 1000 °C is about 18.5 μm, and the thickness of the corrosion products of the modified coating deposited at 1050 °C is about 9.8 μm, indicating that the thermal corrosion resistance of the three groups of yttrium-modified aluminide coating is better than that of the single aluminide coating. Compared with the three groups of modified coatings, the thermal corrosion resistance of yttrium-modified aluminate coating deposited at 1050 °C is better than that of the modified coating deposited at 1000 °C, and both are better than that of the modified coating deposited at 950 °C.

Yttrium can improve the toughness of the coating, thus effectively slowing down the cracking and falling off of the oxide film. Moreover, the yttrium can inhibit the outward diffusion of Cr, Ti, and other elements, and inhibit the inward diffusion of S, thus improving the thermal corrosion resistance of the coating. The higher the content of yttrium, the better the thermal corrosion resistance of the coating.

Figure 14 shows the surface morphology of the (a) single aluminide coating and yttrium-modified aluminide coatings deposited at (b) 950 °C, (c) 1000 °C, and (d) 1050 °C on the K444 alloy after corrosion at 900 °C-Na_2SO_4 + NaCl for 75 h. The single aluminide coating has corrosion holes, and the yttrium-modified coating deposited at 950 °C has corrosion pits, while the samples deposited at 1000 °C and 1050 °C have dense surface coatings without obvious defects. Table 3 shows the surface scan element content of single aluminide coating and three groups of yttrium-modified aluminide coating on K444 alloy after corrosion at 900 °C-Na_2SO_4 + NaCl for 75 h that are corresponded to Figure 14a–d. By synthesizing Figure 14 and Table 3, it can be found that S (0.33 wt.%) and a small number of matrix elements (0.23 wt.% W and 0.29 wt.% Ta) were detected on the surface of the single aluminide coating. It may have internal vulcanization, and the local damage of the coating is relatively serious. The S element (0.28 wt.%) was detected on the surface of the yttrium-modified aluminide coating deposited at 950 °C, but no matrix element is detected. The thermal corrosion resistance of the coating is better than that of the single aluminide coating. The surface of the modified coating deposited at 1000 °C is mainly Al_2O_3 and TiO_2, with a small amount of Cr_2O_3, and no S is found, indicating that the coating has a certain degree of damage, but it still has a good protective effect. The surface of the sample

deposited at 1050 °C is mainly Al_2O_3, with a small amount of TiO_2 and Cr_2O_3, indicating that the coating is not corroded and has good thermal corrosion resistance.

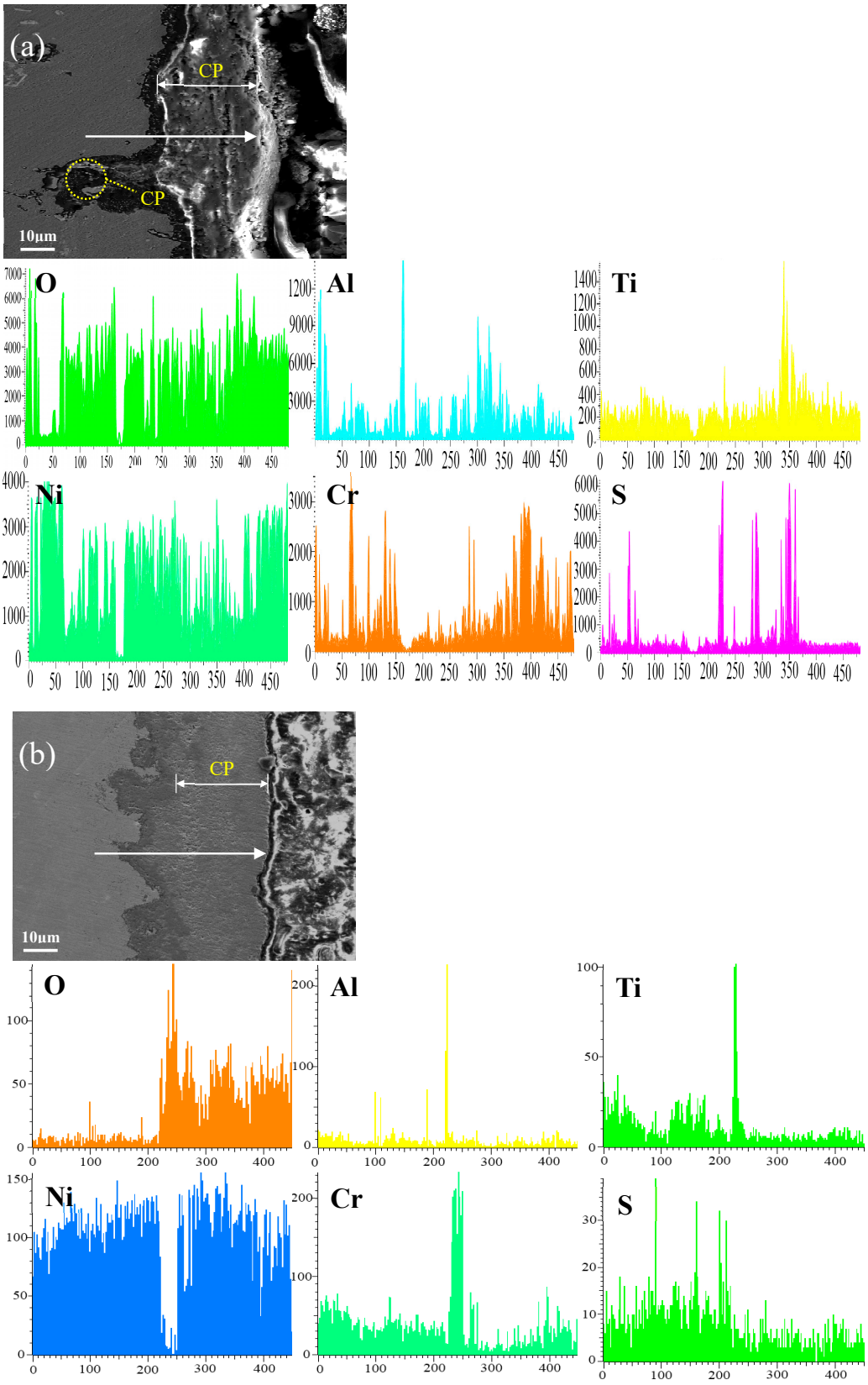

Figure 12. *Cont.*

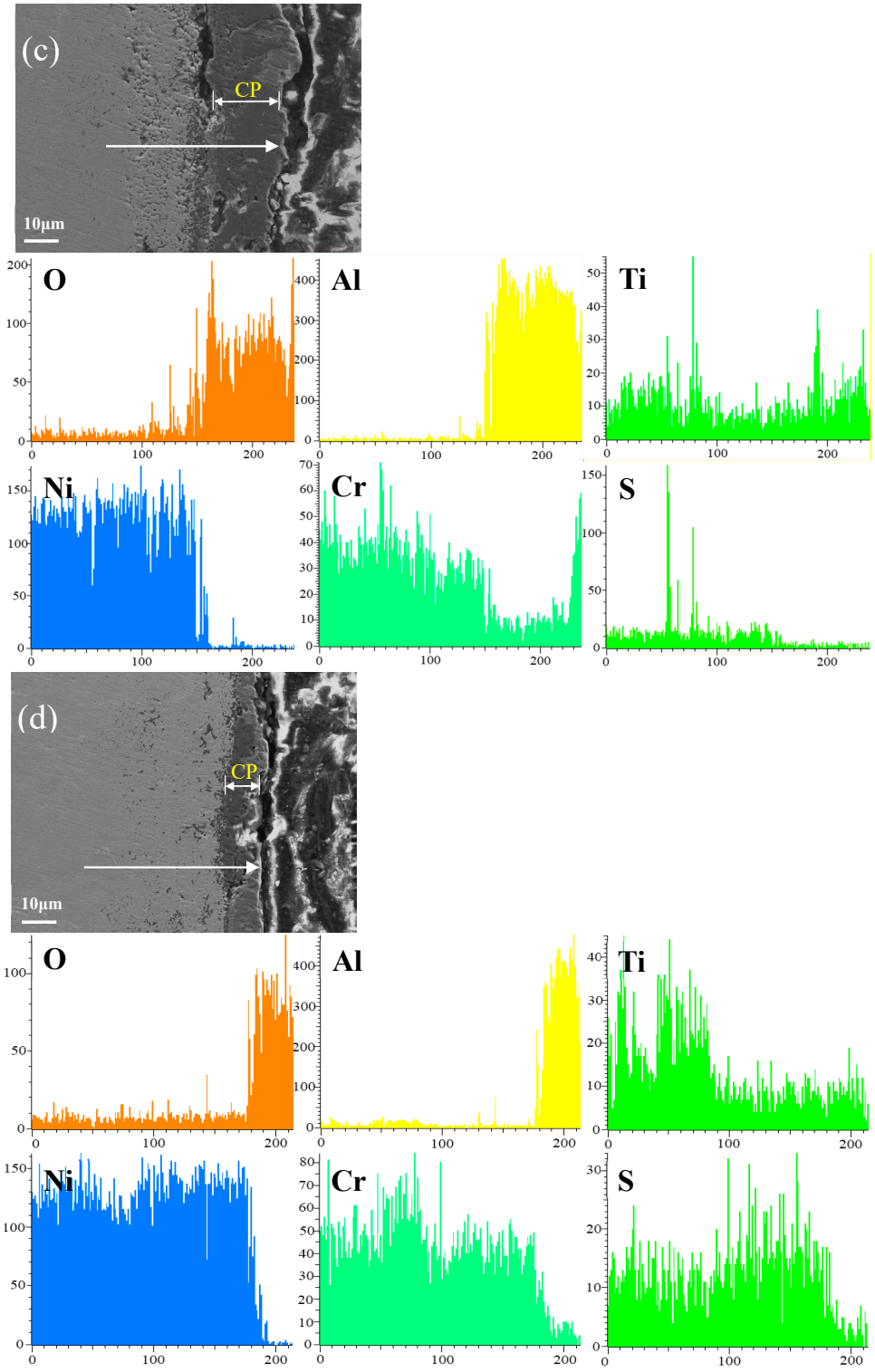

Figure 12. Cross-sectional microstructure of (**a**) single aluminide coating and yttrium-modified aluminide coatings deposited at (**b**) 950 °C, (**c**) 1000 °C, and (**d**) 1050 °C and element line scan maps of Al, Ti, O, Ni, Cr, S on K444 alloy after corrosion at 900 °C-Na_2SO_4 + NaCl for 75 h.

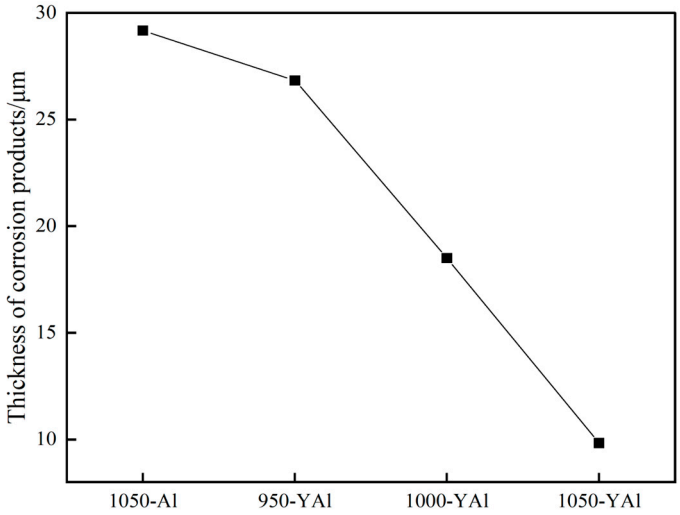

Figure 13. Thickness curves of corrosion products of single aluminide coating and three groups of yttrium-modified aluminide coatings on K444 alloy after corrosion at 900 °C-Na_2SO_4 + NaCl for 75 h.

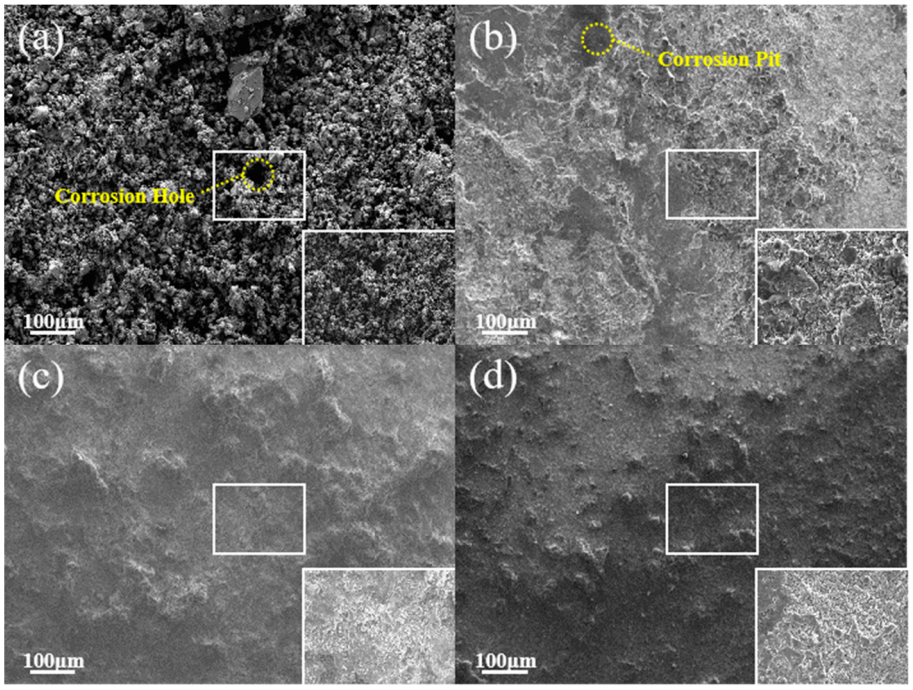

Figure 14. Surface morphologies of (**a**) single aluminide coating and yttrium-modified aluminide coatings deposited at (**b**) 950 °C, (**c**) 1000 °C, and (**d**) 1050 °C on K444 alloy after corrosion at 900 °C-Na_2SO_4 + NaCl for 75 h.

Table 3. Surface scan element content of single aluminide coating and three groups of yttrium-modified aluminide coatings on K444 alloy after corrosion at 900 °C-Na_2SO_4 + NaCl for 75 h (wt.%).

Element / Point	O	Al	Ni	Cr	Ti	Co	S	Residual
Figure 14a	47.61	7.68	24.75	12.81	1.30	5	0.33	0.23 W, 0.29 Ta
Figure 14b	63.95	7.54	12.92	29.09	5.73	8.14	0.28	—
Figure 14c	67.12	25.75	0.51	1.45	4.58	—	—	—
Figure 14d	61.38	35.62	0.58	1.19	1.23	—	—	—

4. Conclusions

(1) Adding yttrium and changing the deposition temperature had no effect on the double-layer structure (outer layer and diffusion layer) of the coating. The addition of yttrium-modified element increased the content of aluminum and the thickness of the coating. When the deposition temperature is 1050 °C and the deposition time is 2 h, the thickness of the yttrium-modified aluminide coating increased by 33%, compared with that of single aluminide coating. Compared with adding yttrium, the deposition temperature has a greater effect on the coating thickness;

(2) The cyclic oxidation test at 1100 °C showed that the high-temperature oxidation resistance of the three yttrium-modified aluminide coatings was better than that of the single aluminide coating. Compared with the three groups of yttrium-modified aluminide coatings, the high-temperature oxidation resistance of the modified coatings deposited at 1000 °C and 1050 °C was close to that of the modified coatings deposited at 950 °C. After cyclic oxidation for 100 h, the single aluminide coating gained 0.55 mg·cm^{-2}, the yttrium-modified aluminide coating deposited at 1050 °C gained 0.3 mg·cm^{-2}, and the oxidation resistance of the coating increased by 45%;

(3) Under the condition of 900 °C-NaCl + Na_2SO_4, the resistance to heat corrosion of the yttrium-modified aluminide coating was better than that of the single aluminide coating. Compared with the three groups of yttrium-modified aluminide coatings, the thermal corrosion resistance of the yttrium-modified aluminide coating deposited at 1050 °C was better than that of the yttrium-modified aluminide coating deposited at 1000 °C, and was superior to the modified coating deposited at 950 °C.

Author Contributions: Conceptualization; investigation, Y.W.; date analysis, S.X.; writing—original draft preparation, H.Y.; methodology; writing—review and editing, Q.S.; supervision; project administration; funding acquisition, F.Y.; data curation, J.D.; software; validation, C.X. All authors have read and agreed to the published version of the manuscript.

Funding: The present study was financed by the National Natural Science Foundation General Program of China (Grant No. 52175182), the Hubei Provincial Natural Science Foundation of China (Grant No. 2022CFB936), the National Key Research and Development Program of China (Grant No. 2020YFB2010400), the Hubei Provincial Key Research and Development Program of China (Grant No. 2021BAA210).

Institutional Review Board Statement: Not applicable.

Informed Consent Statement: Not applicable.

Data Availability Statement: Data are contained within the article.

Conflicts of Interest: All authors were employed by China Academy of Machinery Wuhan Research Institute of Materials Protection Co., Ltd.

References

1. Fan, X.L.; Li, D.J.; Lv, B.W.; Fang, Y.; Zhao, S.Q.; Zhang, W.X.; Wang, T.J. Advances in the fundamentals of the manufacture of industrial gas turbine. *China Basic Sci.* **2018**, *20*, 32.
2. Gao, S.; Hou, J.; Yang, F.; Wang, C.; Zhou, L. High Temperature Oxidation Behaviors of Two Cast Ni-based Superalloys. *Rare Met. Mater. Eng.* **2019**, *48*, 960–966.
3. Yang, H.B.; Wang, Y.S.; Wang, X.; Wu, Q. Research progress of hot corrosion and protection technology of gas turbine under marine environment. *Surf. Technol.* **2020**, *49*, 163.
4. Jiang, C.Y.; Feng, M.; Chen, M.H.; Chen, K.; Geng, S.J.; Wang, F.L. Corrosion behaviour of iron and nickel aluminide coatings under the synergistic effect of NaCl and water vapour. *Corros. Sci.* **2021**, *187*, 109484. [CrossRef]
5. Guo, J.T.; Zhou, L.Z.; Yuan, C.; Hou, J.S.; Qin, X.Z. Microstructure and properties of several originally invented and unique superalloys in China. *Chin. J. Nonferrous Met.* **2011**, *21*, 237–250.
6. Möhwald, K.; Maier, H.J. Thermally Sprayed Nickel-Based Repair Coatings for High-Pressure Turbine Blades: Controlling Void Formation during a Combined Brazing and Aluminizing Process Nicolaus Martin. *Coatings* **2021**, *11*, 725–728.
7. Kanesund, J.; Brodin, H.; Johansson, S. Hot corrosion influence on deformation and damage mechanisms in turbine blades made of IN-792 during service. *Eng. Fail. Anal.* **2019**, *96*, 118. [CrossRef]

8. Yang, S.S.; Yang, L.L.; Chen, M.H.; Wang, J.L.; Wang, F.H. Understanding of failure mechanisms of the oxide scales formed on nanocrystalline coatings with different Al content during cyclic oxidation. *Acta Mater.* **2021**, *205*, 116576. [CrossRef]
9. Pillai, R.; Dryepondt, S.; Armstrong, B.L.; Lance, M.J.; Muralidharan, G.M. Evaluating the efficacy of aluminide coatings to improve oxidation resistance of high performance engine valve alloys. *Surf. Coat. Technol.* **2021**, *421*, 127401. [CrossRef]
10. Kukla, D.; Kopec, M.; Kowalewski, Z.L.; Politis, D.J.; Jóźwiak, S.; Senderowski, C. Thermal Barrier Stability and Wear Behavior of CVD Deposited Aluminide Coatings for MAR 247 Nickel Superalloy. *Materials* **2020**, *13*, 3863. [CrossRef]
11. Kukla, D.; Kopec, M.; Wang, K.; Senderowski, C.; Kowalewski, Z.L. Nondestructive Methodology for Identification of Local Discontinuities in Aluminide Layer-Coated MAR 247 during Its Fatigue Performance. *Materials* **2021**, *14*, 3824. [CrossRef]
12. Góral, M.; Pytel, M.; Kubaszek, T.; Drajewicz, M.; Simka, W.; Nieużyła, Ł. The new concept of thermal barrier coatings with Pt + Pd/Zr/Hf-modified aluminide bond coat and ceramic layer formed by PS-PVD method. *High Temp. Mater. Process.* **2021**, *40*, 281–286. [CrossRef]
13. Qiao, M.; Zhou, C. Codeposition of Co-Al-Y on nickel base superalloys by pack cementation process. *Corros. Sci.* **2013**, *75*, 454–460. [CrossRef]
14. Liu, Z.; Zhou, C. Hot Corrosion Behavior of Si–Y–Co-Modified Aluminide Coating Exposed to NaCl + Na_2SO_4 Salt at 1173 K. *Oxid. Met.* **2016**, *85*, 205–217. [CrossRef]
15. Zielińska, M.; Zagula-Yavorska, M.; Sieniawski, J.; Filip, R. Microstructure and Oxidation Resistance of an Aluminide Coating on the Nickel Based Superalloy Mar M247 Deposited by the CVD Aluminizing Process. *Arch. Metall. Mater.* **2013**, *58*, 697–701. [CrossRef]
16. Dun, Y.Z.; Li, X.J.; Liu, L.; Wu, Y.; Zhang, L.; Xia, S.Y. Preparation of Yttrium Modified Aluminide Coating by Chemical Vapor Deposition Method and Evaluation of Its Performance. *Mater. Prot.* **2018**, *51*, 6–11+39. (In Chinese)
17. *HB 5258-2000*; Determination Method for Oxidation Resistance of Steels and High Temperature Alloys. AVIC CHINA AERO-POLYTECHNOLOGY ESTABLISHMENT: Beijing, China, 2000; pp. 10–12.
18. *HB 20401-2016*; Test for Corrosion Behaviors at High-Temperature with Corrosive Salts. AVIC CHINA AERO-POLYTECHNOLOGY ESTABLISHMENT: Beijing, China, 2016; pp. 1–4.
19. Romanowska, J. Aluminum diffusion in aluminide coatings deposited by the CVD method on pure nickel. *Calphad* **2014**, *44*, 114–118. [CrossRef]
20. Yang, J.; Heogh, W.; Ju, H.; Kang, S.; Jang, T.; Jung, H.; Jahazi, M.; Han, S.C.; Park, S.J.; Kim, H.S.; et al. Functionally graded structure of a nitride-strengthened Mg_2Si-based hybrid composite. *J. Magnes. Alloys* **2024**, *12*, 1239–1256. [CrossRef]
21. Fan, Q.X.; Jiang, S.M.; Yu, H.J.; Gong, J.; Sun, C. The isothermal and cyclic oxidation behavior of two Co-modified aluminide coatings at high temperatures. *Corros. Sci.* **2014**, *84*, 42–53. [CrossRef]
22. Liu, Z.; Zhao, X.; Zhou, C. Improved hot corrosion resistance of Y–Ce–Co-modified aluminide coating on nickel base superalloys by pack cementation process. *Corros. Sci.* **2015**, *92*, 148–154. [CrossRef]
23. Li, S.; Xu, M.M.; Zhang, C.Y.; Niu, Y.S.; Bao, Z.B.; Zhu, S.L.; Wang, F.H. Co-doping effect of Hf and Y on improving cyclic oxidation behavior of (Ni, Pt)Al coating at 1150 C. *Corros. Sci.* **2021**, *178*, 109093. [CrossRef]
24. Zhao, X.; Zhou, C. Effect of Y_2O_3 content in the pack on microstructure and hot corrosion resistance of Y–Co-modified aluminide coating. *Corros. Sci.* **2014**, *86*, 223–230. [CrossRef]